

Received September 22, 2019, accepted October 16, 2019, date of publication October 23, 2019, date of current version November 4, 2019.

Digital Object Identifier 10.1109/ACCESS.2019.2948989

# Using the 0-1 Test for Chaos in Nonlinear Continuous Systems With Two Varying Parameters: Parallel Computations

MACIEJ WALCZAK<sup>1</sup>, WIESLAW MARSZALEK<sup>1</sup><sup>2</sup>, AND JAN SADECKI<sup>2</sup>

<sup>1</sup>SP ZOZ, ZOZ Głucholazy (Hospital), 48-340 Głucholazy, Poland

<sup>2</sup>Institute of Computer Science, Opole University of Technology, 45-758 Opole, Poland

Corresponding author: Wieslaw Marszalek (w.marszalek@po.edu.pl)

**ABSTRACT** Two-parameter diagrams obtained through the 0–1 test of chaos for nonlinear oscillatory continuous systems are presented in this paper. The diagrams are the results of a parallel approach to tackle enormous memory and computational time requirements due to the known oversampling problem associated with the use of the 0–1 test for chaos in continuous systems. Our rectangular diagrams with black-and-white shades of gray levels correspond to the numbers between 0 and 1 obtained as the result of the 0–1 test for chaos. A comparison between the two-parameter diagrams for the 0–1 test with the color bifurcation diagrams for oscillatory systems obtained from another method (*period-n* identification) is also considered. Illustrative examples are based on both the well-known Lorenz model and a model describing two equivalent electric arc circuits.


**INDEX TERMS** The 0–1 test of chaos, two-parameter bifurcation diagrams, oscillatory continuous dynamics, parallel computation, electric arc circuits.

## I. INTRODUCTION

The 0–1 test for chaos is a computational tool to analyze nonlinear dynamical systems based on their time series responses [1]–[5]. Mathematical model of the system is not needed in the analysis. If such a model is known, then one can generate a time series response and feed it into the 0–1 test for chaos. The purpose of the test is to differentiate between periodic and chaotic responses. Typical situation is that a dynamical system is periodic for a particular interval of parameter values while chaotic for others. The well-known Lorenz, Rössler and Chua systems are examples of such continuous nonlinear systems or circuits. Time series periodic and chaotic signals can also be analyzed by other available tools, such as, for example, Lyapunov exponents, Fourier transforms, bifurcation diagrams, return maps, and others [6], [7], [14]. The 0–1 test for chaos is a relatively new test that can be applied to both continuous and discrete nonlinear systems or their time series responses. However, because of the possibility for a time series to be oversampled, the continuous case seems to be more challenging than the discrete one [3]. The oversampling phenomenon has been analyzed in [13] and

its relation to the Fourier spectrum of the time series has been established.

In this paper we further analyze the use of the 0–1 test for chaos in the case when two parameters of a continuous nonlinear system vary slowly, yielding oscillatory time series of various properties. It is quite common in nonlinear systems and circuits that changing one particular element (i.e. a resistor) results in a change of the values of two, three or more parameters (coefficients) in the underlying mathematical model. See, for example, [15] showing an example of a nonlinear circuit in which one resistor value impacts two parameters of the circuit's model, while another resistor impacts three parameters simultaneously. Thus, varying many parameters in mathematical models of nonlinear systems or circuits is a quite natural scenario. Varying slowly two parameters, say  $a$  and  $b$ , with small step sizes  $\Delta a$  and  $\Delta b$ , within certain interval values,  $a_{min} \leq a \leq a_{max}$ ,  $b_{min} \leq b \leq b_{max}$ , may result in a two-dimensional (rectangular) diagram in which each of the hundred of thousand (or even a few million) of discrete pairs of parameter values  $(a_i, b_j)$  is assigned a particular number  $0 \leq K_{i,j} \leq 1$  from the 0–1 test for chaos, or a specific colorbar is used, describing the nature of the response for each of those pairs of parameter values. The later type of two-parameter color diagrams are typical in

The associate editor coordinating the review of this manuscript and approving it for publication was Bing Li .

such an analysis [16], [18]–[20]. The novelty of this paper is that the former type of two-parameter diagrams, obtained from the 0–1 test for chaos with two varying parameters, has not yet been considered in the literature and this paper attempts to report on such two-parameter diagrams for the 0–1 test, their computations and comparison with the later type of diagrams.

The first of two important features of using the 0–1 test for chaos is a necessity of analyzing time-series responses hundred of thousand or a few million of times, as each of the integer indices  $i$  and  $j$  above typically runs up to, or even exceeds, the value of  $10^3$  (depending on  $\Delta a$  and  $\Delta b$ ), giving a matrix of  $10^3 \times 10^3$  values of  $(a_i, b_j)$ . If a continuous nonlinear model is available, then such a model is solved about  $10^6$  times, and for each of the million times the 0–1 test of chaos is applied.

The second important feature is that in many cases of nonlinear continuous chaotic systems and circuits the time horizon of each of the  $10^6$  solutions must be large enough, due to the oversampling problem and one needs to use time series of suitable lengths, to assure that the 0–1 test is applied in a meaningful way, and the obtained  $K_{i,j}$  values fully characterize the nature of the response under consideration. When the underlying mathematical model (system of ordinary differential equations, or ODEs) is solved numerically and the time series is available at certain  $n \cdot dt$  instants ( $n = 0, \dots, n_{final}$ ), then to feed the time series values into the 0–1 test, one needs to use every  $T$  instant, where the positive integer  $T$  depends on the system being analyzed. Thus, the time series at time instants  $n \cdot T \cdot dt$  is used in the 0–1 test. Examples reported in [13], [21] show that the values of  $T$  could range from a single integer value ( $T = 7$  in [13]) to thousands ( $T = 3000$  in [21]). The danger is, that the oversampling phenomenon in the 0–1 test, when not properly addressed (incorrect value of  $T$  chosen), may give incorrect results of the 0–1 test for chaos [22], [23].

Our analysis applies to the following scenarios. First, we assume that a mathematical model of a continuous dynamical process is available in the form of a system of ordinary differential equations (ODEs). The system is solved by a numerical solver with constant or variable step size and an output is created at uniform spacing, say  $0, dt, 2dt, 3dt, \dots$ . A possible example of such a case is to use any numerical ODE solver in Matlab with the **options** feature, as in the following hypothetical sequence which yields a time series (solution of an ODE system) at time instants with constant step  $dt$ , initial condition  $[0.5, 4, 1]$  for  $0 \leq t \leq 500$ :

```
dt = 0.001;
options = odeset('RelTol',1e-8,'AbsTol',[1e-8 1e-8
1e-8]);
```

```
[t,x] = ode45(@f,0:dt:500,[0.5; 4; 1],options);
```

where **@f** is a Matlab function for the analyzed ODE system. See Appendices A and B for a relevant example.

Because of the above two features, obtaining two-parameter diagrams by using the 0–1 test for chaos is rather time consuming with significant memory requirements.

Therefore, our diagrams are obtained using parallel computing, as it is practically impossible to obtain such diagrams using a single processor computing.

The paper is organized as follows. Section 2 describes the results of using the 0–1 test for chaos when one parameter is changed only. The ‘false-negative’ and ‘false-positive’ outcomes of the 0–1 test are described and a ‘false-negative’ outcome is illustrated based on the chaotic Lorenz system. Then, two-parameter diagrams obtained for a relatively simple continuous model of electric arc circuits are presented in section 3. Those two-parameter diagrams are obtained using parallel computation described in section 4. Both software and hardware details of our computations are provided. Next, a comparison between the two-parameter diagrams obtained from the 0–1 test and the traditional color bifurcation diagrams reported in [21] for the same circuits, is presented in section 5. Conclusions and final remarks are given in section 6. Appendices A and B complete the whole presentation.

## II. THE 0–1 TEST FOR CHAOS WITH ONE VARYING PARAMETER

### A. PRELIMINARIES

When one parameter, say  $R$ , in a mathematical model of a nonlinear system (for example described by a system of ODEs), varies in certain interval, then one may obtain the  $K$  values from the 0–1 test for chaos as is shown in Fig.1(a). The parameter  $R$  is the resistance value in the simple arc circuits shown in Fig.2, whose mathematical model is given in Appendix B (see (2)). Thus, for any fixed value of  $R$  in the interval  $[5, 25]$  we obtain the corresponding  $K$  value from the interval  $[0, 1]$ . The values of  $K$  close to 0 indicate periodic time series, while those close to 1 are obtained for chaotic ones. Transition from the values close to 0 to 1 (or vice-versa) are sometimes obtained almost instantly, as, for example, for the  $R$  values in the narrow interval marked by the letter  $\gamma$  in Fig.1(a), or for  $R \approx \delta$ ,  $R \approx \epsilon$  and  $R \approx \zeta$ . For other larger intervals of  $R$  the transition from the values close to 0 to those close to 1 is not as sharp, and several windows of very narrow lengths with values  $K \approx 0$  occur in the interval of increasing values of  $K : 0 \rightarrow 1$ , as in the interval  $9 < R < 13.8$ . The first part of that interval is due to the period doubling bifurcation (approximately from  $R = 9$  to  $R = 10.3$ ). Then, at the value of  $R = \beta$  we obtain a purely periodic time series, so  $K$  drops to the value close to 0.

The 0–1 test for chaos does not differentiate between various types of periodic time series. For example, for  $R = 5$  we have a *period-1* time series, while at the value of  $R \approx \alpha$ , we have a *period-2* time series.<sup>1</sup> Also, the 0–1 test does not give the local maximum values in various *period-n* oscillations as does the corresponding bifurcation diagram shown in Fig.1(b). This bifurcation diagram was obtained by a conventional analysis of oscillatory systems based on

<sup>1</sup>*Period-n* time series has  $n$  local maximum values in one period of oscillations.

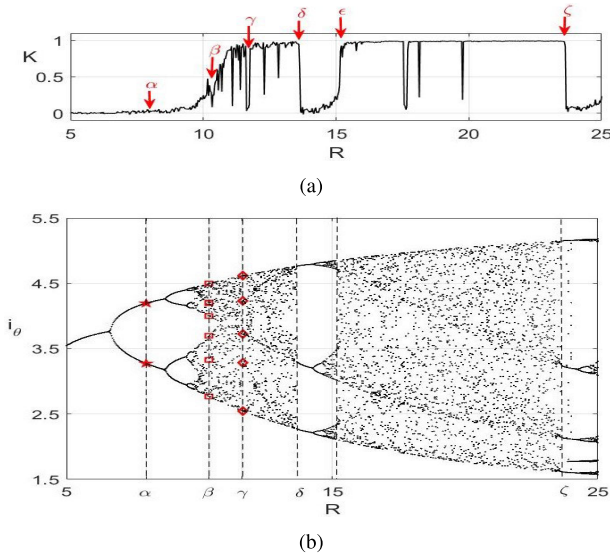


FIGURE 1. (a)  $K$  values from the 0-1 test. (b) the corresponding 1D bifurcation diagram.

identification of the number and values of maximum points in oscillatory systems. Based on Fig. 1(b) one can easily estimate the values of the two local maximum values (in one period) of variable  $i_\theta$  for  $R = \alpha$ , six local maximum values for  $R = \beta$ , and five local maximum values for  $R = \gamma$ . These three cases illustrate the *period-2*, *period-6* and *period-5* oscillations of  $i_\theta$ , respectively.

**B. THE ‘FALSE-NEGATIVE’ AND ‘FALSE-POSITIVE’ OUTCOMES OF THE 0-1 TEST**

Problems with using the 0-1 test were observed, well documented and could be summarized by the footnote quote from [22].<sup>2</sup> The footnote quote continues with the following statement: “...our negative results do not invalidate the 0-1 test as a proper mathematical test for distinguishing regular motion from fully developed chaotic motion. We believe that so long as the system under study is truly deterministic and the motion is far away from the boundary between chaos and regular motions, the test is valid.”

Unfortunately, the above statement is not quite correct. The problems with weak chaos and stochastic noise are only a part of the wider array of problems with the 0-1 test. Another issue that may lead to erroneous results of the 0-1 test is the *oversampling* phenomenon [1], [16]. Even when the system or signal is deterministic and the motion is far away from the boundary between chaos and regular motion, the 0-1 test may incorrectly classify a chaotic motion as regular and, vice versa, a regular system or signal may be classified as a chaotic one. Paper [16] showed examples when a periodic signal

<sup>2</sup>“By studying three different types of data, (i) edge of chaos, (ii) weak chaos, and (iii)  $1/f^\alpha$  noise with long-range correlations, we have shown that the 0-1 test for chaos misclassifies deterministic and weakly stochastic edge of chaos and weak chaos as regular motions, while strongly stochastic edge of chaos and weak chaos, as well as  $1/f^\alpha$  noise, as deterministic chaos.”

TABLE 1. Results of 0-1 test for Lorenz system:  $\sigma = 10, \rho = 28, \beta = 8/3$ . The ‘false-negative’ outcomes correspond to the combination of  $dt$  and  $T$  values with outputs written in the red color.

dt					T
0.005	0.01	0.02	0.04	0.08	
-0.0202	-0.0131	-0.0250	0.1190	0.9963	1
-0.0094	-0.0144	0.0738	0.9954	0.9986	2
-0.0158	0.1340	0.9948	0.9975		4
0.1950	0.9767	0.9960			8
0.9830	0.9980				12
0.9953	0.9981				16
0.9981					20
0.9975					24
0.9981					28
0.9979					32

with multiple frequencies in its spectrum can be erroneously classified as a chaotic with the  $K$  parameter from the 0-1 test being close to 1. This is the case of ‘false-positive’ outcome. It as also shown in [2], [16] that the typical chaotic systems of Lorenz, Rössler and Chua, may be classified as periodic by the 0-1 test, even when other tools (i.e. Lyapunov exponents, power spectrum) indicate otherwise.

*Example:* Consider the coefficients  $K$  shown in Table 1 that were obtained from the 0-1 test applied to various solutions of the Lorenz system having its coefficients  $\sigma = 10, \rho = 28$  and  $\beta = 8/3$ , initial condition  $[10^{-10}, 0, 1]$  with various  $dt$  values and the `ode45` solver. It is well-known that the Lorenz system is chaotic for the chosen values of  $\sigma, \rho$  and  $\beta$ . The solutions were output using `tspan=[0:dt:800]` and the `options` feature. Then, the last 5000 solution values were inserted into the 0-1 test. The  $K$  values from the 0-1 test are shown in the first row in Table 1 (for  $T = 1$ ). Next, again, we considered a sequence of the last 10001 solution values and skipped every other value to form a new sequence of 5000 solutions values. Such a sequence was fed into the 0-1 test. The test results are shown in the second row (for  $T = 2$ ). Following the same pattern, we considered the last 20,000 solution values, skipped every fourth solution value to form another sequence of 5000 solution values to be tested by the 0-1 test again. The results are shown in the third row in Table 1 (for  $T = 4$ ). The empty entries in Table 1 do not exist, since the respective combination of the  $dt$  and  $T$  values do not allow for a creation of a sequence of 5000 values for the time interval  $0 \leq t \leq 800$ . For example, if  $dt = 0.08$ , then  $800/0.08 = 10,000$ , so only 10,001 discrete solution values are available. The last 5000 values are fed into the 0-1 test if  $T = 1$ , while the whole sequence but one value is used when  $T = 2$ . The cases with  $T > 2$  are not possible (see the  $dt = 0.08$  column in Table 1 with no entries for  $T > 2$ ). Notice that all the entries in Table 1 written in red indicate periodic solutions (since  $K \approx 0$ ), and, therefore, the corresponding cases are clearly of the ‘false-negative’ nature. The 0-1 test fails to provide correct answers in those cases. On the other hand,

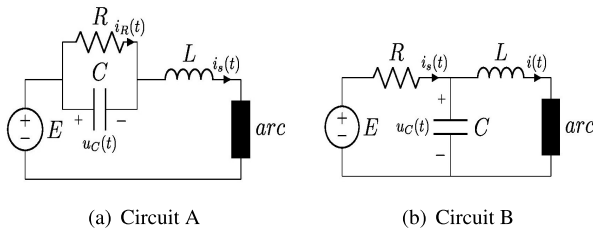


FIGURE 2. Two electric arc circuits.

the cases corresponding to the values written in bold (black color) represent the correct outcomes that could be marked as ‘true-positive’. In those cases the nature of the solutions is correctly identified as chaotic (since  $K \approx 1$ ).

### III. THE 0–1 TEST FOR CHAOS WITH TWO VARYING PARAMETERS

The nonlinear circuits shown in Fig.2 have been recently analyzed in [14] where their 1D and color 2D bifurcation diagrams were obtained through the identification of the number of local maximum values in one period of oscillation. When the number of such maximum values exceeded 16 or the circuit’s response was chaotic for certain pairs of two parameter values, then such cases were assigned the white color. *Period-1* through *period-15* oscillations were marked through a colorbar ranging from dark brown to light yellow colors. Similar approach was used elsewhere [15]–[21], where the rectangular color bifurcation diagrams were reported.

Based on the equivalence between the results of the 0–1 test and 1D bifurcation diagrams illustrated through the graphs in Fig.1, one expects a similar correspondence in the 2D (two-parameter) case. When two parameters (any pair of the three parameters  $R$ ,  $L$  and  $C$ ) in (2) vary simultaneously, then the 0–1 test for chaos results in a matrix, possibly of very large size (say,  $10^3 \times 10^3$ ) with the values  $0 \leq K_{i,j} \leq 1$ . Then, one simply obtains a discrete 2D function  $f(i,j) = K_{i,j}$  with  $K_{i,j} \approx 0$  for *period- $n$*  response (with  $n$  being a natural number), while  $K_{i,j} \approx 1$  for chaotic response. In this paper, the interval  $[0, 1]$  of possible  $K_{i,j}$  values has been divided into 256 levels  $k/255$ ,  $k = 0, 1, \dots, 255$ , and for each entry of  $K_{i,j}$  one of those 256 gray levels has been assigned. The black color represents  $K_{i,j} = 0$ , white color is for  $K_{i,j} = 1$ , and the remaining values of  $K_{i,j} = \{1/255, 2/255, \dots, 254/255\}$  are represented by the remaining 254 shades of gray.

The two-parameter bifurcation diagrams obtained from the 0–1 test for chaos have not been reported in the literature. This paper shows such diagrams for the circuits in Fig.2 with 256 gray levels of  $K_{i,j}$  between 0 and 1. The two-parameter diagrams are presented for various three sizes:  $300 \times 300$ ,  $600 \times 600$  and  $2000 \times 2000$  discrete points of  $(L_i, C_j)$  or  $(C_i, R_j)$ . Moreover, our two-parameter diagrams are compared with the diagrams obtained by another method of computing such diagrams that is based on the identification of the number  $n$  in the *period- $n$*  oscillations or a failure to identify  $n$  when chaotic responses occur. In particular, for the circuits

in Fig.2 we identify periodic oscillations with the value of  $n$  from 1 to as high as 64. Another novelty of this paper is an analysis of parallel computation of the two-parameter diagrams for the 0–1 test as we provide the values of the parallel efficiency coefficients and parallel computing times in comparison to the sequential (single processor) computations. Our analysis can be applied to any other oscillatory circuit or system described by sets of nonlinear ODEs of various sizes.

## IV. PARALLEL COMPUTATION OF BIFURCATION DIAGRAMS WITH TWO VARYING PARAMETERS

### A. SOFTWARE AND HARDWARE USED

To reduce the computing time burden and high memory requirements when solving the ODE system (2) hundred of thousand (or a few million) times and performing the 0–1 test for chaos in the two-parameter case, the Intel Phi MIC (Many Integrated Core) architecture and parallel computing were utilized. The computer system had 3 Intel Xeon Phi Coprocessor 7120 units, each equipped with 61 cores clocking 1.238 GHz frequency. Individual core enabled running maximally 4 threads, which, as a consequence, made an execution of 244 threads on one card possible. The code launched on one core could be executed sequentially as well as by using a 2-piped processing. In order to maximize the computational capabilities of the Intel Phi MIC architecture, it is advisable to run at least two threads on one core, so that the 2-piped processing is implemented. Each card was fitted with 16 GB RAM GDDR5 memory, while the communication with other devices and cards was being performed by the PCI bus.

The Intel MIC architecture was installed on the mainboard Supermicro X10DRG-OT+–CPU with two Intel Xeon E5-2650 v3 2.30GHz processors and 112 GB RAM memory. The operating system managing co-processors was 64-bit Ubuntu 14.04.5 LTS, while the installed cards were shared as three Linux hosts working in TCP/IP network. Our computations of two-parameter diagrams require both the high CPU performance and significant amount of RAM memory. For solving a nonlinear system of three ODEs with the chosen Runge-Kutta method of order 4, integration step  $dt = 0.001$  in the interval  $t \in [0, 10000]$ , with each of the coprocessors running 120 threads, the size of allocated memory should be equal  $(10000/0.001) \cdot 120 \cdot 8 \cdot 3 = 28.8$  GB, where 8 bytes is used for storing a double precision floating point number. The 0–1 test was being run only on one of the vectors so the value of 28.8 GB could be reduced to 9.6 GB, which is still quite big, and in the case of using a smaller integration step  $dt$  or larger than 10,000 seconds of time interval of solving of ODEs, becomes an issue. Since the 0–1 test is using a vector of 5000 time samples, the needed memory amount can be minimalized to the value of  $5000 \cdot 120 \cdot 8 = 4.8$  MB, regardless of the integration step size and length of the interval of integration.

The application was written in the C language and, to obtain a parallel effect, the Intel MPI and OpenMP were



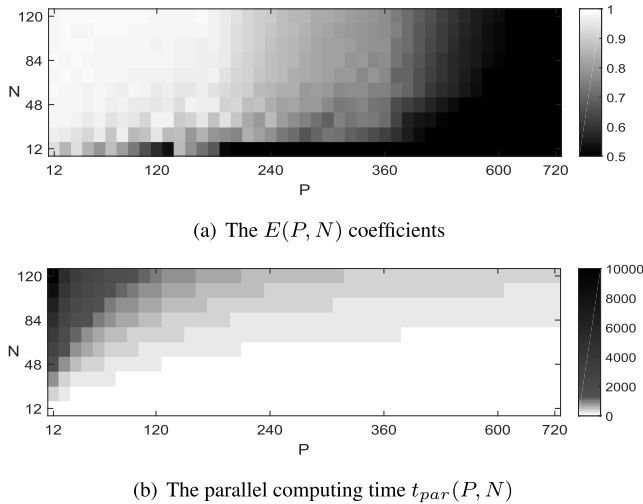


FIGURE 3. The  $E(P, N)$  coefficients and time computing  $t_{par}(P, N)$  values.

used. Also, the Intel C++ Compiler (icc) supporting the MIC architecture was used. A programmer has an option to use the Intel MKL (Mathematical Kernel Library), too. The use of MKL will certainly improve code performance, but that was not a goal set in this paper.

In order to create the bifurcation diagrams in this paper an algorithm with parallelization on two levels was used. The first parallelization takes place on the node level (3 coprocessors), while the second parallelization is done on the level of individual nodes. A creation of a  $600 \times 600$  diagram (consisting of 360000 discrete points) was statically divided between 3 nodes, each of which performed parallel computing for 120000 points of the diagram. Next, the resulting matrix was assembled on the main node. Depending on the way in which the task was divided and on the implemented mechanisms, the application was built into three versions, (1) through (3), as follows:

- (1): level 1 - MPI static task allocation, level 2 - MPI static task allocation,
- (2): level 1 - MPI static task allocation, level 2 - OpenMP static task allocation,
- (3): level 1 - MPI static task allocation, level 2 - OpenMP dynamic task allocation.

The entire task, comprising  $N^2$  diagram points, was divided into  $P = P_1 \cdot P_2$  parallel tasks, where  $P_1$  and  $P_2$  are the numbers of coprocessors and processes (or threads) running on coprocessors, respectively. In the versions (2) and (3) above it is necessary to consider both local and global variables, whereas version (1) implements local variables only. The additional asset of version (3) is the OpenMP scheduling for the main loop, where the pool of  $N^2/P_1$  tasks is assigned to  $P_2$  threads dynamically. After performing computations by individual nodes, the results are assembled by the MPI on the main node.

The objective of the following part of this section is to demonstrate effectiveness of the parallel implementation in

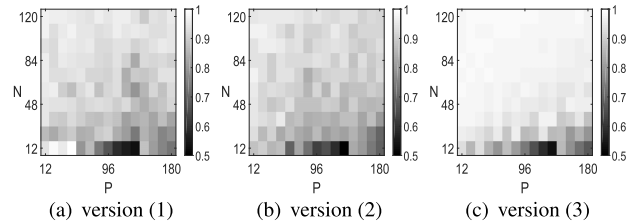


FIGURE 4. The  $E(P, N)$  efficiency coefficients for parallel computation.

comparison to the sequential algorithm, as well as to illustrate how the effectiveness depends on the way in which the coprocessor architecture is used. In addition, the effectiveness of the above mentioned three application models is examined. For comparison, the following *efficiency coefficient* was defined and used

$$E(P, N) = \frac{t_{seq}(1, N)}{t_{par}(P, N) \cdot N} \quad (1)$$

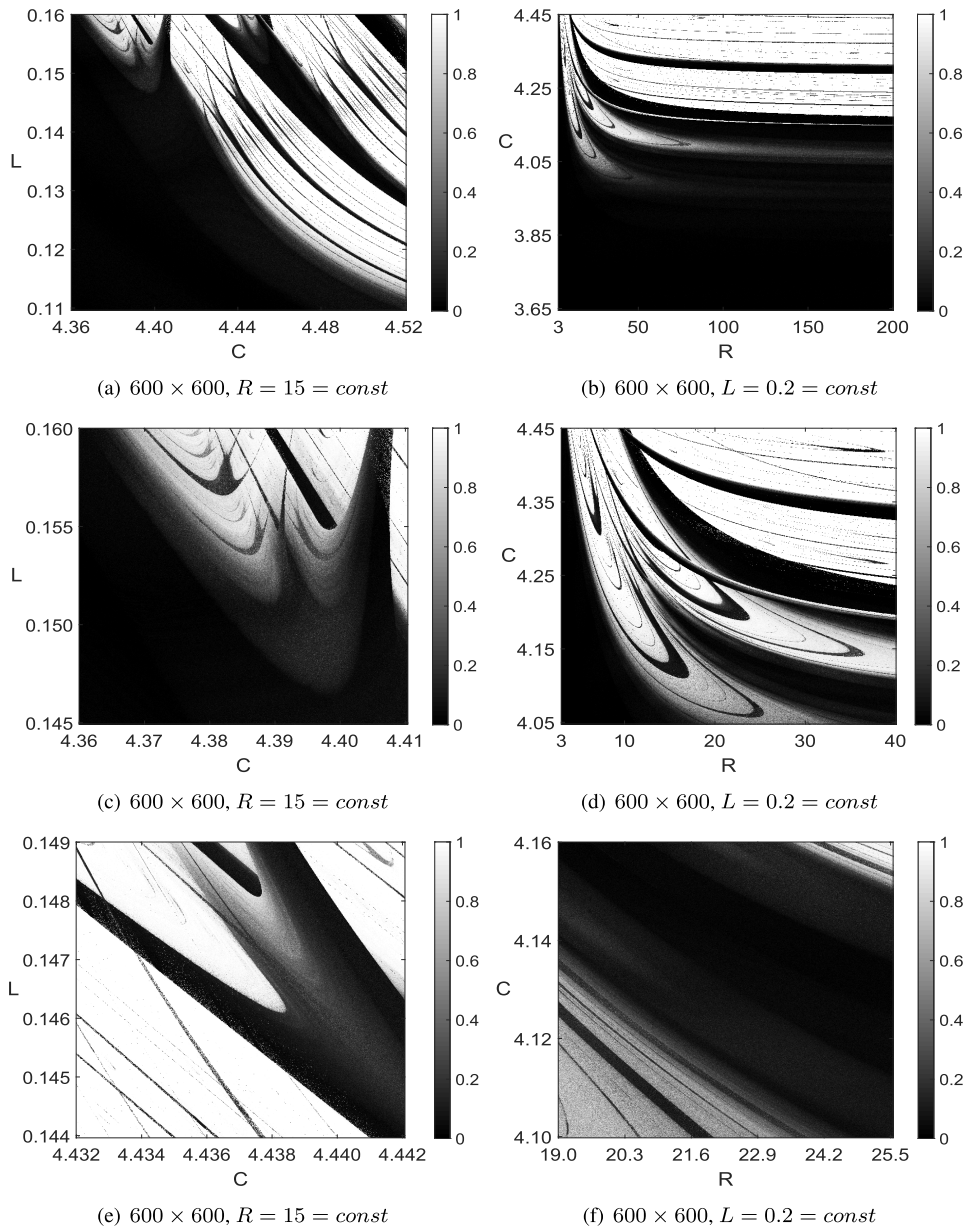
where  $P$  is the number of parallel processes or threads (we use the word threads from now on),  $N$  is the size of the task (diagrams are of  $N \times N$  size),  $t_{seq}(1, N)$  is the time of completing a task of size  $N$  by one thread, while  $t_{par}(P, N)$  is the time of completing the same task of size  $N$  by  $P$  parallel threads. The coefficient (1) is a number from the interval  $(0, 1)$ , reaching higher values for better parallelization effectiveness. Due to the fact that obtaining  $t_{seq}(1, N)$  for large  $N$  is extremely difficult, if not impossible, (for  $600 \times 600$  diagrams it requires about 840 hours of computation), it was assumed that  $t_{seq}(1, N) = t_{seq}(1, 1) \cdot N$ . Thus, (1) simplifies to  $E(P, N) = t_{seq}(1, 1)/t_{par}(P, N)$ . For estimating  $t_{seq}(1, 1)$ , 100 measurements of the time computing were performed and the mean of  $t_{seq}(1, N) = 8.3723$  seconds with standard deviation of  $\sigma = 0.0149$  seconds was obtained.

Fig.3 shows the  $E(P, N)$  coefficients and  $t_{par}(P, N)$  (in seconds) computing times depending on the size  $N$  and the number of threads  $P$ . The computations were done by version (3), see above, where each task is performed with the use of

- individual coprocessor cores for  $P \in [12, 180]$ ,
- 1-2 logical cores for  $P \in (180, 360]$ , and
- 3-4 logical cores for  $P \in (360, 720]$ .

In Fig.3(a) a nonlinear scale was used, where for  $P \in [12, 360]$  a measurement with the step size of  $12 \cdot P$  was implemented, whereas for  $P \in (360, 720]$  the size of  $24 \cdot P$  was used. To illustrate the difference in  $t_{par}(P, N)$  computing time a nonlinear gray scale was applied in Fig.3(b).

It can be noticed that the most effective parallelization appears when  $P \in [12, 180]$ , where for  $N > 36$  the coefficients  $E$  are high with  $E(P, N)_{N>36} = 0.976$ . Relatively high coefficients  $E(P, N)$  together with short computation times are observed when  $P \in (180, 360]$ . On the other hand, the shortest computations are obtained when the number of threads is close to 720 and all logical cores are involved. In this case the coefficients  $E(P, N)$  are the lowest ones. As a result, there is a little time saving in the case when



**FIGURE 5.** Two-parameter  $600 \times 600$  diagrams obtained with the 0–1 test for chaos with  $T = 1700$  and  $dt = 0.001$ .

$P \in (180, 360]$ . This fact is illustrated in Fig.3(b), where, for  $N = 120$  the gray levels change significantly for  $P \in (12, 360]$ , but there is practically no difference for  $P \in (360, 720]$ .

From the three analyzed implementations, version (3) (based on dynamic tasks scheduling OpenMP and MPI distribution) was proved to be the most beneficial. The effectiveness of particular implementation for  $P \in \{12, 24 \dots, 180\}$  and  $N \in \{12, 24, \dots, 120\}$  was analyzed as shown in Fig. 4. The values of coefficient  $E$  for the implementation versions (1) and (2) are similar and the mean values equal  $\overline{E(P, N)}_{(1)} = 0.8999, \overline{E(P, N)}_{(2)} = 0.8883$  and  $\overline{E(P, N)}_{(3)} = 0.9452$ , respectively.

Both the parallel mechanisms and the way in which the computer architecture is used impact the computing time. In all implementations, the task scheduling between the three coprocessors was static. For size  $N$  with  $N^2 \bmod 3 \neq 0$ , the coprocessors were assigned different numbers of tasks. This has an impact on the parallel efficiency coefficients. The optimal results are delivered through the use of dynamic scheduling on the second level of parallelization. A similar effect is expected when the task scheduling is done dynamically also on the first level. The key  $600 \times 600$  diagrams for the 0–1 test for chaos presented in this paper were created by version (3) described above. The  $t_{par}(P, 600), P = 180, 360, 720$ , and  $t_{par}(720, 2000)$  computing times and

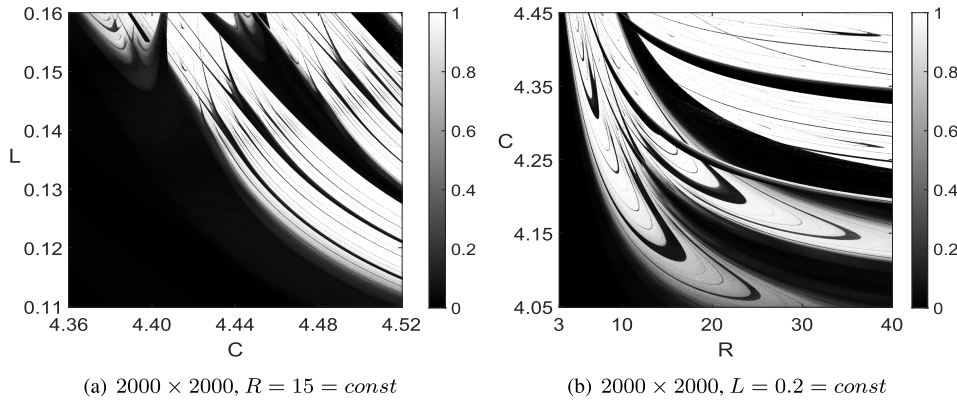


**FIGURE 6.** Two  $2000 \times 2000$  two-parameter diagrams obtained with the 0-1 test for chaos. They correspond to the diagrams shown in Fig.5(a) and Fig.5(d), respectively.  $T = 1700$  and  $dt = 0.001$  for both diagrams.

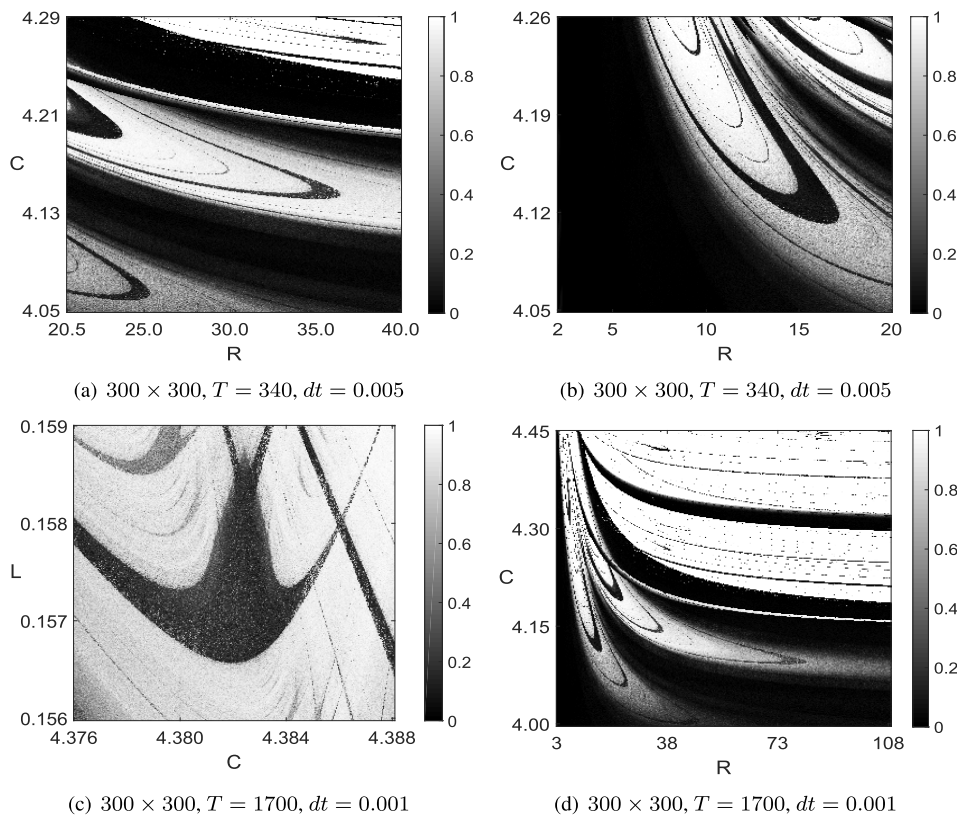


**FIGURE 7.** Various  $300 \times 300$  two-parameter diagrams obtained with the 0-1 test for chaos.  $L = 0.2 = const$  for diagrams (a), (b) and (d), while  $R = 15 = const$  for diagram (c).

$E(P, 600)$ ,  $P = 180, 360, 720$ , and  $E(720, 2000)$  coefficients were obtained as follows:

- $t_{par}(180, 600) = 16984.7383$  seconds (4.72 hours),  $E(180, 600) = 0.9857$ ,
- $t_{par}(360, 600) = 10478.9354$  seconds (2.91 hours),  $E(360, 600) = 0.7990$ ,
- $t_{par}(720, 600) = 8691.8441$  seconds (2.41 hours),  $E(720, 600) = 0.4816$ ,
- $t_{par}(720, 2000) = 96234.9790$  seconds (26.731 hours),  $E(720, 2000) = 0.4833$ .

It can be noticed that the coefficient  $E(180, 600)$  is close to 1. Around 98.6% of the coprocessor time was used for computations, while the remaining 1.4% was used for the parallelization mechanisms. The granulation of the tasks minimized the use of synchronization mechanism and access to the critical section. Moreover, the dynamic allocation of the tasks on the second parallelization level improved the overall efficiency of computations. Notice the difference between the coefficients  $E(P, 600)$  and the close values of  $t_{par}(360, 600)$  and  $t_{par}(720, 600)$  above.



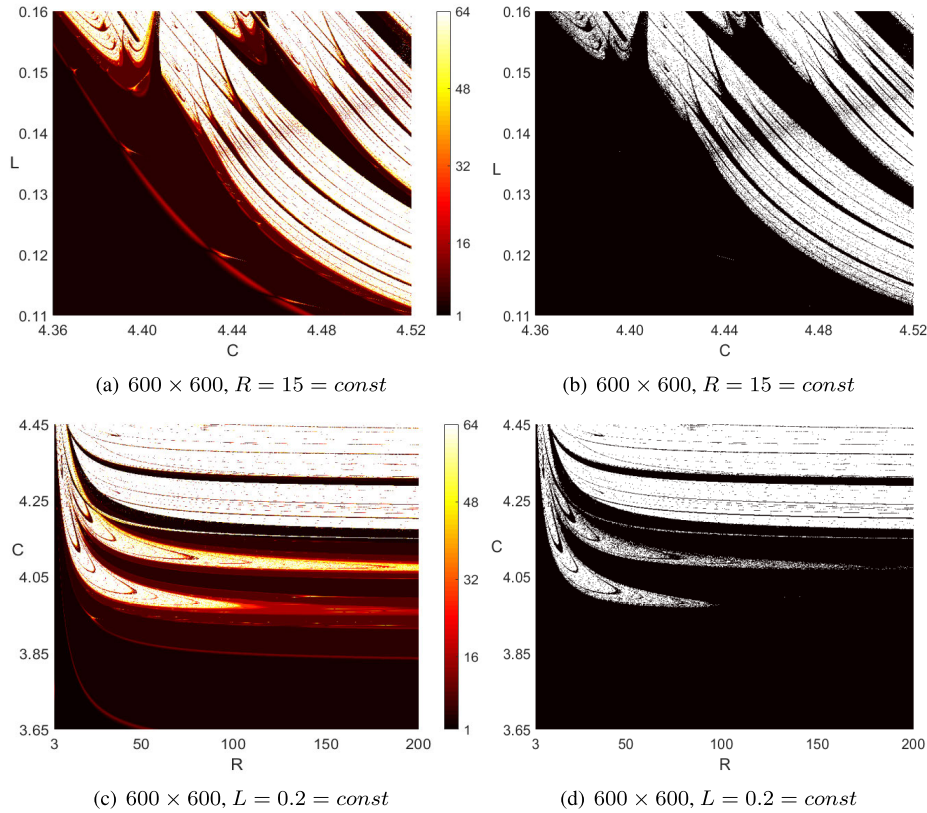


**FIGURE 8.** First part of a two-part figure (with Fig.9). For an extensive caption see Fig. 9. The above four diagrams correspond to the diagrams in Figs.5(a) and 5(b).

**B. RESULTS OF NUMERICAL EXPERIMENTS: PROPERTIES OF TWO-PARAMETER DIAGRAM FOR THE 0-1 TEST**

Figs.5, 6 and 7 show the two-parameter diagrams for the 0-1 test for chaos when the pairs of parameters  $(L, C)$  and  $(C, R)$  vary. The gray level bars with 256 levels (from the black level corresponding to  $K = 0$  to the white level corresponding to  $K = 1$ ) are shown on the right-hand side of each diagram. Figs.5(c) and 5(e) on the left-hand side correspond to two zoomed-in rectangles in Fig.5(a). Similarly, Figs.5(d) and 5(f) on the right-hand side correspond to two zoomed-in rectangles in Fig.5(b). Any sharp edge in those diagrams - a rapid change between the white and black colors, or equivalently from the values  $K \approx 1$  to  $K \approx 0$ ) shows a dramatic change from a chaotic response to a periodic one - as, for example, for the values of  $R = \delta$  and  $R = \zeta$  in Fig.1. Notice the relatively high value of parameter  $T$  used in most of the two-parameter diagrams in Figs.5, 6 and 7. The value of  $T$  chosen according to the recommendation of [13], depends, in general, on the nonlinear system of ODEs, and for a particular system, on the step of integration  $dt$ . From the qualitative point of view, even observed with a naked human eye, the diagrams in Figs.5, 6, 7(c) and 7(d) have the product  $T \cdot dt = 1700 \cdot 0.001 = 1.7$  and exactly the same product  $T \cdot dt = 340 \cdot 0.005 = 1.7$  is for the diagrams in Figs.7(a) and 7(b).

Notice also, that the two  $2000 \times 2000$  diagrams shown in Figs.6(a) and 6(b) correspond to the  $600 \times 600$  diagrams

in Figs.5(a) and 5(d), respectively. Although each of the former two diagrams required solutions of  $4 \cdot 10^6$  systems (2) and each of the later two diagrams required only  $3.6 \cdot 10^5$  solutions (ratio of the number of solved systems is about 11.1), there is a very little difference in the quality of the two sets of diagrams under comparison. Obviously, a slightly worse *granulation* is observed in Figs.5(a) and 5(d) than in Figs.6(a) and 6(b), but the difference is difficult to be observed with a naked human eye.

**V. COMPARISON WITH ANOTHER TEST FOR CHAOS**

In this section we compare the two-parameter diagrams obtained for the 0-1 test for chaos applied to system (2), as described in the previous two sections, with the corresponding two-parameter diagrams obtained by the method described in [15]. Identification of the value of  $n$  in any *period-n* oscillatory response results in color two-parameter diagrams shown in Figs.8(a), 8(c) and Figs.9(a), 9(c). The black color corresponds to  $n = 1$ , that is *period-1* oscillations, while the light yellow color represents  $n = 63$ , that is *period-63* oscillations. The periodic oscillations with  $n \geq 64$  and chaotic oscillations are represented by the white color at the top of the color bars on the right sides of the color diagrams. The color diagrams in Figs.8(a), 8(c) correspond to the diagrams for the 0-1 test in Figs.5(a), 5(b), respectively. Also, the color diagrams in Figs.9(a), 9(c) correspond to the diagrams for the 0-1 test Figs.5(c), 5(d), respectively.



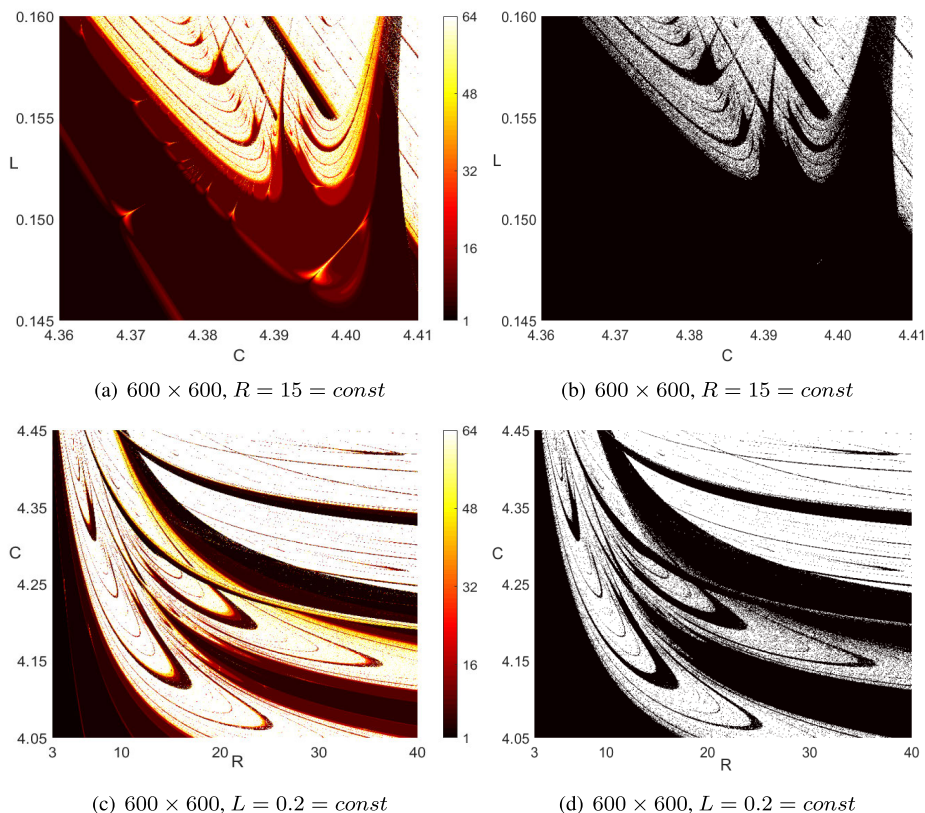


**FIGURE 9.** Second part of the two part figure (with Fig.8). Figs.8 and 9 show various  $600 \times 600$  two-parameter diagrams obtained with the identification of the maximum values of the periodic responses (up to 63 maximum values in one period) and assigning the value  $n = 64$  and the white color for other responses (including chaotic ones). System (2) was solved for  $0 \leq t \leq 4000$  with integration step  $dt = 0.001$ . Identification of maximum points done for  $2000 \leq t \leq 4000$ . Color diagrams on the left hand side represent periodic solutions with the number of maximum points in one period from 1 (*period-1* oscillations) to 63 (*period-63* oscillations), while all periodic oscillations with 64 or more maximum points in one period and chaotic solutions are represented by the white color. For the black-and-white diagrams on the right hand side the black color represents all periodic solutions from *period-1* to *period-63* oscillations, and the remaining solutions are represented by the white color. The above four diagrams correspond to the diagrams in Figs.5(c) and 5(d).

The parameters used in obtaining the color diagrams in Figs.8(a), 8(c) and Figs.9(a), 9(c) were: step of integration  $dt = 0.001$  (the same as in computation of most of the diagrams using 0–1 test for chaos), time interval of computation  $t \in [0, 4000]$  seconds, time period for finding the maximum values and identification of the type of *period- $n$* ,  $n = 1, \dots, 63$  (or assigning  $n = 64$  (white color)), was  $2000 \leq t \leq 4000$  seconds (half of the interval of solution). Also, the color diagrams in Figs.8(a), 8(c) and Figs.9(a), 9(c) were obtained by parallel computing method, different than the one described in Section 4 of the present paper. In the method of identification of the values of maximum points the issue of oversampling does not occur, so the solutions required significantly shorter time intervals than in the case of the 0–1 test for chaos. However, other issues need to be considered that do not appear in the 0–1 test for chaos. For example, the issue of accuracy of numerical identification of the maximum points in one period is important. In general, making a comparison between the two methods of identifying periodic and chaotic solutions is difficult, if not impossible. Also, in this paper we identified periodic solutions up to *period-63*, while assigning

$n = 64$  for all other periodic solutions and chaotic ones. On the other hand, the  $K$  values obtained from the 0–1 test for chaos were digitized at 256 gray levels. The binary black-and-white diagrams in Figs.8(b), 8(d) as well as in Fig.9(b), 9(d) were obtained from their respective color counterparts on the left side, by assigning the black color to all *period-1* through *period-63* solutions, while the white color is assigned to the solutions with  $n = 64$ , as explained before. Those black-and-white diagrams in Figs.8(b), 8(d) as well as Fig.9(b), 9(d) agree extremely well with the diagrams obtained with the 0–1 test for chaos, that is the diagrams in Figs.5(a), 5(b) as well as in Figs.5(c), 5(d). The method used to compute the color diagrams in Figs.8(a), 8(c), 9(a) and 9(c) is described in details in [15].

## VI. CONCLUSION

Parallel computations of two-parameter bifurcation diagrams for the 0–1 test for chaos were presented in this paper. Due to enormous memory requirement and computation time burden it is practically impossible to obtain such diagrams using single processor computation. Effectiveness of parallel

computation has also been analyzed from the point of view of the size  $N \times N$  of the computed diagrams and the value of  $P$ , the number of threads. Moreover, the obtained two-parameter diagrams were compared with the corresponding diagrams obtained by a conventional method of analyzing periodic and chaotic diagrams, based on the identification of *period-n* responses (for  $n = 1, \dots, 63$ ) through the maximum values in one period or determination that  $n \geq 64$ , for which the white color is assigned in the color bifurcation diagrams. It is also possible to compare out approach to the 0-1 test for chaos and two-parameter bifurcation diagrams with similar diagrams for the largest Lyapunov exponents. Our illustrative examples utilize a nonlinear ODE model for two equivalent electric arc circuits. The method presented in this paper is applicable to any nonlinear dynamical system whose mathematical model is based on nonlinear ODEs. Each such a system, for example considered in [24]–[26], [28], has its own proper combination of the  $dt$  and  $T$  parameters that should be examined before the 0-1 test is applied.

**APPENDIX A  
AN ODE SYSTEM IN MATLAB FOR THE ELECTRIC ARC  
CIRCUITS IN APPENDIX B**

The code below shows `@f` for the circuits described in Appendix B below and the dimensionless system of three ODEs on the right-hand side of (2).

```
function xdot = f(t,x)
global R
m = -2/3; C = 3.14; L = 1;
xdot(1) = (1/L)*(x(2)-x(1))*(x(3)^m);
xdot(2) = (1+R-x(2)-R*x(1))/(R*C);
xdot(3) = x(1)^2-x(3);
xdot = xdot';
end
```

**APPENDIX B  
THE CIRCUITS AND THEIR MODEL [14]**

The electric arc circuit in Fig.2(a) is described by the system of three equations on the left side of (2) below and its dimensionless version on the right side [21]

$$\begin{aligned} \frac{di}{d\tau} &= \frac{1}{L}(u_C - \frac{U(i_\theta)}{i_\theta}i) & \frac{dx}{dt} &= \frac{1}{L}(y - xz^m) \\ \frac{du_C}{d\tau} &= \frac{1}{RC}(E - u_C - Ri) \rightarrow \frac{dy}{dt} &= \frac{1}{RC}(R + 1 - y - Rx) \\ \frac{di_\theta^2}{d\tau} &= \frac{1}{\theta}(i^2 - i_\theta^2) & \frac{dz}{dt} &= x^2 - z \end{aligned} \quad (2)$$

where  $x = i/I_0$ ,  $y = u_C/U_0$ , and  $z = i_\theta^2/I_0^2$ , with  $i_\theta$  being the arc current,  $i$  and  $u_C$  denoting the current through  $L$  and voltage across  $C$ , respectively (see Fig.1(a)). The  $U_0$  and  $I_0$  are constants from the *static* arc volt-ampere characteristic  $U(i_\theta) = U_0(i_\theta/I_0)^n$  with  $n < 0$ . This means that the voltage across the element representing the arc column in Fig.1(a) is  $U(i_\theta)i/i_\theta$ , which follows from the dynamic and static relations in the welding arcs - see [29] for more details. The  $\theta = \tau/t$ ,  $L$ ,  $C$  and  $R$  are the time constant, inductance,

capacitance and resistance, respectively. The  $m$  in (2) is such that  $-1 < m = (n - 1)/2 < 0$  and, typically,  $m = -2/3$ , which follows from  $U(i_\theta) = i_\theta^n$ , with  $n = -1/3$ . Also, one may consider the system on the right side in (2) as the system on the left side with  $U_0 = I_0 = \theta = 1$  and the fact that  $E = RI_0 + U_0$ . The circuit in Fig.2(b) is also described by (2) with an appropriate change of variables [29].

It can be shown that (2) has two equilibrium points:  $(1, 1, 1)$  and  $(x_a, x_a^n, x_a^2)$ , where  $x_a$  is the solution of  $1 + R - Rx_a - x_a^n = 0$ . The second equilibrium is unstable provided that  $R + n > 0$ , which is assumed to be satisfied in this paper. Qualitative analysis of the two equilibrium points, the associated eigenvalues and Hopf bifurcations of (2) are derived in the case of 1D bifurcations in [29] and an interesting link between AC models of electric arcs and memristors is discussed in [30].

**ACKNOWLEDGMENT**

The authors would like to thank the three anonymous reviewers for their helpful and constructive comments.

**REFERENCES**

- [1] G. A. Gottwald and I. Melbourne, "Testing for chaos in deterministic systems with noise," *Phys. D, Nonlinear Phenomena*, vol. 212, nos. 1-2, pp. 100-110, 2005.
- [2] G. A. Gottwald and I. Melbourne, "On the implementation of the 0-1 test for chaos," *SIAM J. Appl. Dyn. Syst.*, vol. 8, no. 1, pp. 129-145, Jun. 2009.
- [3] G. A. Gottwald and I. Melbourne, "The 0-1 test for chaos: A review," in *Chaos Detection and Predictability (Lecture Notes in Physics)*, vol. 915, C. Skokos, G. Gottwald, and J. Laskar, Eds. Berlin, Germany: Springer, 2016.
- [4] G. Litak, A. Syta, and M. Wiercigroch, "Identification of chaos in a cutting process by the 0-1 test," *Chaos, Solitons Fractals*, vol. 40, pp. 2095-2101, Jun. 2009.
- [5] M. A. Savi, F. H. I. Pereira-Pinto, F. M. Viola, A. S. de Paula, D. Bernardini, G. Litak, and G. Rega, "Using 0-1 test to diagnose chaos on shape memory alloy dynamical systems," *Chaos, Solitons Fractals*, vol. 103, pp. 307-324, Oct. 2017.
- [6] Q. Xu, Y. Lin, B. Bao, and M. Chen, "Multiple attractors in a non-ideal active voltage-controlled memristor based Chua's circuit," *Chaos, Solitons Fractals*, vol. 83, pp. 186-200, Feb. 2016.
- [7] C. Xu and Y. Wu, "Bifurcation and control of chaos in a chemical system," *Appl. Math. Model.*, vol. 39, no. 8, pp. 2295-2310, 2015.
- [8] M. Melosik and W. Marszalek, "Using the 0-1 test for chaos to detect hardware trojans in chaotic bit generators," *Elect. Lett.*, vol. 52, no. 11, pp. 919-921, May 2016.
- [9] B. Bao, N. Wang, Q. Xu, H. Wu, and Y. Hu, "A simple third-order memristive band pass filter chaotic circuit," *IEEE Trans. Circuits Syst. II, Exp. Briefs*, vol. 64, no. 8, pp. 977-981, Aug. 2017.
- [10] I. M. Wangari, S. Davis, and L. Stone, "Backward bifurcation in epidemic models: Problems arising with aggregated bifurcation parameters," *Appl. Math. Model.*, vol. 40, no. 2, pp. 1669-1675, 2016.
- [11] D. Castano, M. C. Navarro, and H. Herrero, "Routes to chaos from axisymmetric vertical vortices in a rotating cylinder," *Appl. Math. Model.*, vol. 54, pp. 1-20, Feb. 2018.
- [12] X. Li, P. Niu, and J. Liu, "Combustion optimization of a boiler based on the chaos and Lévy flight vortex search algorithm," *Appl. Math. Model.*, vol. 58, pp. 3-18, Jun. 2018.
- [13] W. Marszalek and M. Melosik, "On the 0/1 test for chaos in continuous systems," *Bull. Polish Acad. Sci., Tech. Sci.*, vol. 63, no. 3, pp. 521-528, 2016.
- [14] W. Marszalek and J. Sadecki, "2D Bifurcations and chaos in nonlinear circuits: A parallel computational approach," in *Proc. 15th Int. Conf. Synth., Modeling, Anal. Simulation Methods Appl. Circuit Design (SMACD)*, Prague, Czech Republic, Jul. 2018, pp. 297-300. doi: 10.1109/SMACD.2018.8434908.

- [15] W. Marszalek and J. Sadecki, "Complex two-parameter bifurcation diagrams of a simple oscillating circuit," *IEEE Trans. Circuits Syst. II, Exp. Briefs*, vol. 66, no. 4, pp. 687–691, Apr. 2019.
- [16] J. G. Freire, R. J. Fields, and J. A. C. Gallas, "Relative abundance and structure of chaotic behavior: The nonpolynomial Belousov-Zhabotinsky reaction kinetics," *J. Chem. Phys.*, vol. 131, no. 4, p. 044105, 2009.
- [17] H. Podhaisky and W. Marszalek, "Bifurcations and synchronization of singularly perturbed oscillators: An application case study," *Nonl. Dyn.*, vol. 69, pp. 949–959, 2012.
- [18] W. Marszalek and H. Podhaisky, "2D bifurcations and Newtonian properties of memristive Chua's circuits," *Europhys. Lett.*, vol. 113, no. 1, p. 10005, 2016.
- [19] M. J. B. Hauser and J. A. C. Gallas, "Nonchaos-mediated mixed-mode oscillations in an enzyme reaction system," *J. Phys. Chem. Lett.*, vol. 5, no. 23, pp. 4187–4193, 2014.
- [20] J. G. Freire, M. R. Gallas, and J. A. C. Gallas, "Nonchaos-mediated mixed-mode oscillations in a prey-predator model," in *Proc. 6th Int. Conf. Nonlinear Sci. Complex. Chaotic, Fractional, Complex Dyn., New Insights Perspect.*, São José dos Campos, Brazil, Springer, 2016, pp. 101–124, 2017.
- [21] W. Marszalek and J. Sadecki, "Parallel computing of 2-D bifurcation diagrams in circuits with electric arcs," *IEEE Trans. Plasma Sci.*, vol. 47, no. 1, pp. 706–713, Jan. 2019.
- [22] J. Hu, W.-W. Tung, J. Gao, and Y. Cao, "Reliability of the 0-1 test for chaos," *Phys. Rev. E, Stat. Phys. Plasmas Fluids Relat. Interdiscip. Top.*, vol. 72, no. 5, p. 056207, 2005.
- [23] P. Matthews. *0-1 Test for Chaos*. Accessed: Mar. 21, 2019. [Online]. Available: <https://www.mathworks.com/matlabcentral/fileexchange/25050-0-1-test-for-chaos>
- [24] T. Chen, L. Huang, P. Yuc, and W. Huang, "Bifurcation of limit cycles at infinity in piecewise polynomial systems," *Nonlinear Anal., Real World Appl.*, vol. 41, pp. 82–106, Jun. 2018.
- [25] Q. Lai, C. Chen, X.-W. Zhao, J. Kengne, and C. Volos, "Constructing chaotic system with multiple coexisting attractors," *IEEE Access*, vol. 7, pp. 24051–24056, 2019.
- [26] Q. Lai, B. Norouzi, and F. Liu, "Dynamic analysis, circuit realization, control design and image encryption application of an extended Lü system with coexisting attractors," *Chaos, Solitons Fractals*, vol. 114, pp. 230–245, Sep. 2018.
- [27] W. Marszalek, H. Podhaisky, and J. Sadecki, "Computing two-parameter bifurcation diagrams for oscillating circuits and systems," *IEEE Access*, vol. 7, no. 1, pp. 115829–115835, 2019.
- [28] G.-H. Xu, Y. Shekofteh, A. Akgül, C.-B. Li, and S. Panahi "A new chaotic system with a self-excited attractor: Entropy measurement, signal encryption, and parameter estimation," *Entropy*, vol. 20, no. 2, p. 86, 2018.
- [29] I. V. Pentegov and V. N. Sydorets, "Comparative analysis of models of dynamic welding arc," *Paton Welding J.*, vol. 12, pp. 45–48, Dec. 2015.
- [30] W. Marszalek and Z. Trzaska, "Dynamical models of electric arcs and memristors: The common properties," *IEEE Trans. Plasma Sci.*, vol. 45, no. 2, pp. 259–265, Oct. 2017.



**MACIEJ WALCZAK** received the M.Sc. degree in computer networks and database management from the Opole University of Technology, Opole, Poland, in 2011, where he is currently pursuing the Ph.D. degree with the Institute of Computer Science. He is currently a Computer Network Administrator with SP ZOZ, ZOZ Głuchołazy (Hospital), Głuchołazy, Poland. His past research interests were in the areas overlapping phenomenon and static optimization using parallel computing. He is currently interested in using parallel computing in the analysis of dynamical systems. In his spare time, he enjoys traveling and reading about astronomy.



**WIESŁAW MARSZAŁEK** received the Ph.D. and D.Sc. degrees in electrical engineering from the Warsaw University of Technology, Poland, and the Ph.D. degree in applied mathematics from North Carolina State University, Raleigh, NC, USA. He was a Humboldt Research Fellow in Bochum (1990–1992), Hamburg (1996), and Halle (2011), all in Germany, and a Fulbright Research Fellow in Warsaw (2005–2006) and Opole (2018), both in Poland. He currently teaches computer science at the Opole University of Technology, Poland, and mathematics at Rutgers University, New Jersey, NJ, USA. He has published over 100 journal and conference papers in the areas of 2D discrete equations, differential-algebraic equations, nonlinear circuits and electric arcs, memristors, and singularity induced bifurcations and chaos.



**JAN SADECKI** received the Ph.D. and D.Sc. degrees in automatic control and robotics from the Warsaw University of Technology, Poland, in 1988 and 2004, respectively. From 1992 to 1993, he spent a sabbatical year at the Centre for Mathematical Software Research, University of Liverpool, U.K. From 2012 to 2016, he was the Associate Chair of the Department of Electrical Engineering. Since 2017, he has been the Director of the Institute of Computer Science, Opole University of Technology. His research and teaching interests are in the areas of parallel computing, and distributed computing networks and optimization.

• • •